

Apparent deviations from causality in spontaneous light emission by atomic hydrogen in the mid- and far-field regions

Vincent Debierre* and Thomas Durt

Aix Marseille Université, CNRS, École Centrale de Marseille, Institut Fresnel UMR 7249, 13013 Marseille, France

(Received 27 August 2015; revised manuscript received 29 December 2015; published 29 February 2016)

We investigate, in the case of the $2P$ - $1S$ transition in atomic hydrogen, the behavior of the spontaneously emitted electromagnetic field in space-time. We focus on Glauber's wave function for the emitted photon, a quantity which we find is nonzero outside the light cone at all times after the start of the emission. We identify the uncertainty on the position of the decaying electron as a source of departure from causality in the naive sense of the term. We carry out a detailed study of the emitted electric field in the mid- and far-field regions, through analytical and numerical computations as well as asymptotic arguments.

DOI: [10.1103/PhysRevA.93.023847](https://doi.org/10.1103/PhysRevA.93.023847)

I. INTRODUCTION

Fermi was the first to study the electromagnetic field emitted during an atomic transition, which has since then been a recurring theme of investigation in atomic physics and quantum electrodynamics [1–5]. Fermi [1] found that, if the survival probability of the electron in the excited state is assumed to decay exponentially, according to the usual Wigner-Weisskopf approximation [6], then the emitted electromagnetic field will propagate causally, in other words, vanish outside the light cone centered around $t = 0$ (the instant at which the emission starts) and the position $\mathbf{x} = \mathbf{0}$ of the hydrogen nucleus (proton). It was then noticed by Shirokov [2] that Fermi's result made use of an approximation, which consisted of extending the range of integration over electromagnetic frequencies from the positive real semiaxis to the whole real axis, thereby including nonphysical electromagnetic negative frequency modes in the treatment. Hegerfeldt later [4] formalized and generalized Shirokov's remarks, linking the absence of negative electromagnetic frequencies with the noncausal field propagation via the Paley-Wiener theorem [7] on holomorphic Fourier transforms.

In contrast to the case of classical electrodynamics where causality can be established by making use of the properties of the retarded Green's functions, there exists no similar rigorous result in the case of quantum electrodynamics (QED). Sipe showed however [5] that, after performing a series of approximations similar to the ones which we will use in Sec. IV, one can approximate the QED description of spontaneous emission by a theory in which the photon wave function obeys (complex) Maxwell-type equations and thus admits a causal (retarded) Green's function. Therefore, we expect that departures from causality will be small in the case of spontaneous emission. Since Sipe's construction is not exact, however, it is not clear at this level whether QED is intrinsically noncausal or whether apparent noncausalities result from approximations performed during the treatment. The goal of our paper is to investigate these questions by making use of the photon wave function [8], which allows us to tackle the problem of causality quantitatively.

Our main new results are the following:

(1) Even if we artificially include negative frequencies, thereby bypassing Hegerfeldt's objections, the photon wave

function is still nonvanishing outside the light cone, which establishes that Hegerfeldt's mechanism is not the single source of noncausality in the present problem. We explain however (Sec. VIB) that this violation is only apparent, namely, that it merely reflects the nonzero spatial extension of the light source, in accordance with Shirokov's predictions [2]. This result follows from a rigorous computation of the single photon wave function, and by the use of exact expressions for the coupling coefficients between electronic $1S$ and $2P$ states of the hydrogen atom and electromagnetic modes [9,10].

(2) We also reconsider Hegerfeldt's paradox by comparing the weight of positive and (virtual) negative electromagnetic frequencies, for different time regimes and distances from the atom. Hegerfeldt's theorem teaches that causality is approximately reached when artificially including negative frequencies in the treatment is a good approximation. We show that this approximation becomes very solid when the dynamics of the emission exits the Zeno regime and enters the Fermi regime, where only field frequencies which are resonant with the atomic transition are excited.

The paper is structured as follows. In Sec. II we review the tools for the description of spontaneous emission. Section III sets the stage for the computation of the wave function of the emitted photon, which is the object which we use in order to assess causality. In Sec. IV we review the usual treatment [1,11] where causality is derived by the way of multiple approximations (dipole approximation, extension of the electromagnetic spectrum to negative frequencies, and use of the usual $\mathbf{E} \cdot \hat{\mathbf{x}}$ coupling instead of the minimal $\mathbf{A} \cdot \hat{\mathbf{p}}$ coupling between the atomic electron and the EM field). In Secs. V and VI we refine the treatment by progressively waiving various approximations, and we find that the result is no longer causal. We identify the different sources of noncausality, and study the space-time dependence of the photon wave function in the mid- and far-field regions in detail. In Sec. VII we study numerically the space-time dependence of the weight of the aforementioned negative frequencies, which constitutes an upper bound on the "weight of noncausality." We conclude in Sec. VIII.

II. DECAY OF A TWO-LEVEL ATOM

Let us consider a two-level atom (ground state $|g\rangle$, excited state $|e\rangle$) interacting with the electromagnetic field. The atom

*vincent.debierre@fresnel.fr

sits in free space. The Hamiltonian $\hat{H} = \hat{H}_A + \hat{H}_R + \hat{H}_I$ is a sum of three terms: the atom Hamiltonian \hat{H}_A , the electromagnetic field Hamiltonian \hat{H}_R , and the interaction Hamiltonian \hat{H}_I . In the Schrödinger picture these read [12]

$$\hat{H}_A = \hbar\omega_g|g\rangle\langle g| + \hbar\omega_e|e\rangle\langle e|, \quad (1a)$$

$$\hat{H}_R = \sum_{\lambda=\pm} \int \tilde{d}k \hbar c ||\mathbf{k}|| \hat{a}_{(\lambda)}^\dagger(\mathbf{k}, t=0) \hat{a}_{(\lambda)}(\mathbf{k}, t=0), \quad (1b)$$

$$\hat{H}_I = \frac{e}{m_e} \hat{\mathbf{A}}(\hat{\mathbf{x}}, 0) \cdot \hat{\mathbf{p}}, \quad (1c)$$

where ω_g (ω_e) is the angular frequency of the ground (excited) atomic level, λ labels the polarization of the electromagnetic field, and m_e is the electron mass. Also, $\hat{\mathbf{x}}$ is the electron position operator and $\hat{\mathbf{p}}$ is the electron linear momentum operator. The field operator $\hat{\mathbf{A}}(\mathbf{x}, t)$ is the vector potential (here we work in the Coulomb gauge), which is expanded over plane waves as

$$\begin{aligned} \hat{\mathbf{A}}(\mathbf{x}, t) = & \sqrt{\frac{\hbar}{\epsilon_0 c}} \sum_{\lambda=\pm} \int \tilde{d}k [\hat{a}_{(\lambda)}(\mathbf{k}, t) \boldsymbol{\epsilon}_{(\lambda)}(\mathbf{k}) e^{i\mathbf{k}\cdot\mathbf{x}} \\ & + \hat{a}_{(\lambda)}^\dagger(\mathbf{k}, t) \boldsymbol{\epsilon}_{(\lambda)}^*(\mathbf{k}) e^{-i\mathbf{k}\cdot\mathbf{x}}]. \end{aligned} \quad (2)$$

Here

$$\tilde{d}k \equiv \frac{d^4k}{(2\pi)^4} 2\pi \delta(k_0^2 - \mathbf{k}^2) \theta(k_0) \quad (3)$$

is the usual volume element on the light cone [13,14] (where θ stands for the Heaviside distribution), which is invariant under Poincaré transformations. The polarization vectors $\boldsymbol{\epsilon}_{(\lambda=\pm)}(\mathbf{k})$ are any two mutually orthogonal unit vectors taken in the plane orthogonal to the wave vector \mathbf{k} . Finally, we give the commutation relation between the photon ladder operators, which reads

$$[\hat{a}_{(\lambda)}(\mathbf{k}), \hat{a}_{(\lambda)}^\dagger(\mathbf{q})] = 2||\mathbf{k}|| (2\pi)^3 \delta(\mathbf{k} - \mathbf{q}) \delta_{\lambda\lambda}. \quad (4)$$

We consider spontaneous emission in a vacuum: at $t = 0$, the electron is in its excited state, while no photons are present in the field. For such an initial condition, the rotating wave approximation holds [15] and the state of the system at time $t \geq 0$ reads

$$\begin{aligned} |\psi(t)\rangle = & c_e(t) e^{-i\omega_e t} |e, 0\rangle \\ & + \sum_{\lambda=\pm} \int \tilde{d}k c_{g,\lambda}(\mathbf{k}, t) e^{-i(\omega_g + c||\mathbf{k}||)t} |g, 1_{\lambda,\mathbf{k}}\rangle, \end{aligned} \quad (5)$$

where $|e, 0\rangle$ means that the atom is in its excited state and the field contains no photons and $|g, 1_{\lambda,\mathbf{k}}\rangle$ means that the atom is in its ground state and the field contains a photon of wave vector \mathbf{k} and polarization λ .

Let us turn to the matrix elements of the interaction Hamiltonian in the Hilbert (sub)space spanned by $|e, 0\rangle$ and $|g, 1_{\lambda,\mathbf{k}}\rangle$. These are well known for the $2P$ - $1S$ hydrogen transition. Writing, for this transition, $|g\rangle \equiv |1S\rangle$ and $|e\rangle \equiv |2P m_2\rangle$, with m_2 the magnetic quantum number of the $2P$

sublevel considered, one has [10]

$$\begin{aligned} \langle 1S, 1_{\lambda,\mathbf{k}} | \hat{H}_I | 2P m_2, 0 \rangle \\ = -i \sqrt{\frac{\hbar}{\epsilon_0 c}} \frac{\hbar e}{m_e a_0} \frac{2^{\frac{3}{2}}}{3^4} \frac{\boldsymbol{\epsilon}_{(\lambda)}^*(\mathbf{k}) \cdot \boldsymbol{\xi}_{m_2}}{[1 + (\frac{2}{3} a_0 ||\mathbf{k}||)^2]^2}, \end{aligned} \quad (6)$$

where we introduced the Bohr radius a_0 . The $\boldsymbol{\xi}_{m_2}$ are given by

$$\boldsymbol{\xi}_0 = \mathbf{e}_z, \quad (7a)$$

$$\boldsymbol{\xi}_{\pm 1} = \mp \frac{\mathbf{e}_x \pm i\mathbf{e}_y}{\sqrt{2}}. \quad (7b)$$

In order to derive (6), one must remember the expressions for the electronic wave functions of the $1S$ and $2P m_2$ sublevels:

$$\psi_{1S}(\mathbf{x}) = \frac{\exp(-\frac{||\mathbf{x}||}{a_0})}{\sqrt{\pi a_0^3}}, \quad (8a)$$

$$\psi_{2P m_2}(\mathbf{x}) = \frac{\exp(-\frac{||\mathbf{x}||}{2a_0}) \sqrt{2}}{8\sqrt{\pi a_0^3}} \frac{\mathbf{x} \cdot \boldsymbol{\xi}_{m_2}}{a_0}. \quad (8b)$$

Since we are interested in spontaneous emission, we set $c_e(t=0) = 1$ and $\forall \lambda \in \{1, 2\} \forall \mathbf{k} \in \mathbb{R}^3 c_{g,\lambda}(\mathbf{k}, t=0) = 0$. We want to compute probability amplitudes of emission, namely

$$c_{g,\lambda}(\mathbf{k}, t) = \langle g, 1_{\lambda,\mathbf{k}} | \hat{U}(t) | e, 0 \rangle, \quad (9)$$

where $\hat{U}(t) = \exp(-i/\hbar \hat{H}t)$ is the evolution operator for the system. From (1) and (5), we get

$$\begin{aligned} \dot{c}_e(t) = & - \sum_{\lambda=\pm} \int \frac{d\mathbf{k}}{(2\pi)^3 2||\mathbf{k}||} \\ & \times G_{\lambda}^*(\mathbf{k}) c_{g,\lambda}(\mathbf{k}, t) e^{-i(c||\mathbf{k}|| - \omega_e + \omega_g)t}, \end{aligned} \quad (10a)$$

$$\dot{c}_{g,\lambda}(\mathbf{k}, t) = -\frac{i}{\hbar} G_{\lambda}(\mathbf{k}) c_e(t) e^{i(c||\mathbf{k}|| - \omega_e + \omega_g)t}, \quad (10b)$$

where $G_{\lambda}(\mathbf{k}) = \langle 1S, 1_{\lambda,\mathbf{k}} | \hat{H}_I | 2P m_2, 0 \rangle$.

III. PHOTON WAVE FUNCTION

The single-photon wave function, hereafter referred to as “the photon wave function,” is a very useful object for the description of one-photon Fock states of the electromagnetic field either in momentum space [16] or, as developed more recently [5,17–19], in direct space (and time). In the rest of the paper, we will use Glauber’s photon wave function to investigate the spontaneous emission of light during the atomic transition at hand, and focus on causality. This wave function was first introduced by Glauber and Titulaer [20] in order to characterize correlations of the electromagnetic field in quantum optics.

Consider a pure, single-photon state of the electromagnetic field

$$|1, f(t)\rangle \equiv \sum_{\lambda} \int \tilde{d}k \tilde{f}_{\lambda}(\mathbf{k}, t) \hat{a}_{(\lambda)}^\dagger(\mathbf{k}) |0\rangle. \quad (11)$$

The photon wave function can be obtained through Glauber’s extraction rule which, when states and operators are defined in

the Schrödinger picture, reads [17–19]

$$\psi_{\perp}(\mathbf{x}, t) = \langle 0 | \hat{\mathbf{E}}_{\perp}(\mathbf{x}, 0) | 1, f(t) \rangle, \quad (12)$$

where $\hat{\mathbf{E}}_{\perp}$ represents the transverse part of the electric-field operator defined through

$$\hat{\mathbf{E}}_{\perp}(\mathbf{x}, t) = i \sqrt{\frac{\hbar c}{\epsilon_0}} \sum_{\lambda=\pm} \int \tilde{d}\mathbf{k} ||\mathbf{k}|| [\hat{a}_{(\lambda)}(\mathbf{k}, t) \boldsymbol{\epsilon}_{(\lambda)}(\mathbf{k}) e^{i\mathbf{k}\cdot\mathbf{x}} - \hat{a}_{(\lambda)}^{\dagger}(\mathbf{k}, t) \boldsymbol{\epsilon}_{(\lambda)}^*(\mathbf{k}) e^{-i\mathbf{k}\cdot\mathbf{x}}]. \quad (13)$$

In our problem, the state of the electromagnetic field is not pure, but rather, as seen from (5), entangled with that of the atom. Hence, projecting onto the single-photon sector and applying Glauber's extraction rule (12), the single-photon wave function reads

$$\begin{aligned} \psi_{\perp}(\mathbf{x}, t) &\equiv \langle g(t), 0 | \hat{\mathbf{E}}_{\perp}(\mathbf{x}, 0) | \psi(t) \rangle = \sum_{\lambda=\pm} \int \tilde{d}\mathbf{k} \langle 0 | \hat{\mathbf{E}}_{\perp}(\mathbf{x}, 0) c_{g,\lambda}(\mathbf{k}, t) e^{-i c ||\mathbf{k}|| t} | 1_{\lambda, \mathbf{k}} \rangle \\ &= i \sqrt{\frac{\hbar c}{\epsilon_0}} \sum_{\lambda=\pm} \int \tilde{d}\mathbf{k} ||\mathbf{k}|| e^{i(\mathbf{k}\cdot\mathbf{x} - c ||\mathbf{k}|| t)} c_{g,\lambda}(\mathbf{k}, t) \boldsymbol{\epsilon}_{(\lambda)}(\mathbf{k}). \end{aligned} \quad (14)$$

A. Formal computation: Preliminary steps

At this point, it comes in handy to notice that (10b) can be formally integrated, yielding

$$c_{g,\lambda}(\mathbf{k}, t) = -\frac{i}{\hbar} \int_0^t dt' G_{\lambda}(\mathbf{k}) c_e(t') e^{i(c ||\mathbf{k}|| - \omega_e + \omega_g)t'}, \quad (15)$$

so that the single-photon wave function reads, in the most general case of our problem,

$$\begin{aligned} \psi_{\perp}(\mathbf{x}, t) &= \sqrt{\frac{c}{\hbar \epsilon_0}} \sum_{\lambda=\pm} \int \tilde{d}\mathbf{k} ||\mathbf{k}|| e^{i(\mathbf{k}\cdot\mathbf{x} - c ||\mathbf{k}|| t)} \boldsymbol{\epsilon}_{(\lambda)}(\mathbf{k}) G_{\lambda}(\mathbf{k}) \int_0^t dt' c_e(t') e^{i(c ||\mathbf{k}|| - \omega_e + \omega_g)t'} \\ &= -i \frac{2^{\frac{9}{2}}}{3^4} \frac{\hbar e}{\epsilon_0 m_e a_0} \sum_{\lambda=\pm} \int \tilde{d}\mathbf{k} ||\mathbf{k}|| e^{i(\mathbf{k}\cdot\mathbf{x} - c ||\mathbf{k}|| t)} \boldsymbol{\epsilon}_{(\lambda)}(\mathbf{k}) \frac{\boldsymbol{\epsilon}_{(\lambda)}^*(\mathbf{k}) \cdot \boldsymbol{\xi}_{m_2}}{[1 + (\frac{||\mathbf{k}||}{k_X})^2]^2} \int_0^t dt' c_e(t') e^{i(c ||\mathbf{k}|| - \omega_0)t'}, \end{aligned} \quad (16)$$

where we introduced $\omega_0 \equiv \omega_e - \omega_g$ and $k_X \equiv 3/(2a_0)$. The unit polarization vectors obey the closure relation

$$\sum_{\lambda=\pm} (\boldsymbol{\epsilon}_{(\lambda)}^i)^*(\mathbf{k}) \boldsymbol{\epsilon}_{(\lambda)}^j(\mathbf{k}) = \delta^{ij} - \frac{k^i k^j}{\mathbf{k}^2} \quad (17)$$

so that the wave function now is

$$\psi_{\perp}(\mathbf{x}, t) = -i \frac{2^{\frac{9}{2}}}{3^4} \frac{\hbar e}{\epsilon_0 m_e a_0} \int \tilde{d}\mathbf{k} ||\mathbf{k}|| \frac{e^{i(\mathbf{k}\cdot\mathbf{x} - c ||\mathbf{k}|| t)}}{[1 + (\frac{||\mathbf{k}||}{k_X})^2]^2} \left(\boldsymbol{\xi}_{m_2} - \frac{\boldsymbol{\xi}_{m_2} \cdot \mathbf{k}}{\mathbf{k}^2} \mathbf{k} \right) \int_0^t dt' c_e(t') e^{i(c ||\mathbf{k}|| - \omega_0)t'}. \quad (18)$$

Choosing a coordinate system for which \mathbf{x} points along the third axis \mathbf{e}_z , we can compute the angular integrals:

$$\begin{aligned} \mathbf{F}(k, ||\mathbf{x}||) &\equiv \int_0^{\pi} d\theta \sin \theta \int_0^{2\pi} d\varphi \left[\boldsymbol{\xi}_{m_2} - \left(\boldsymbol{\xi}_{m_2} \cdot \frac{\mathbf{k}}{||\mathbf{k}||} \right) \frac{\mathbf{k}}{||\mathbf{k}||} \right] e^{ik ||\mathbf{x}|| \cos \theta} \\ &= \int_0^{\pi} d\theta \sin \theta e^{ik ||\mathbf{x}|| \cos \theta} \int_0^{2\pi} d\varphi \left\{ \begin{bmatrix} \xi_{m_2}^{(x)} \\ \xi_{m_2}^{(y)} \\ \xi_{m_2}^{(z)} \end{bmatrix} - \begin{bmatrix} \sin \theta \cos \varphi \\ \sin \theta \sin \varphi \\ \cos \theta \end{bmatrix} \left(\xi_{m_2}^{(x)} \sin \theta \cos \varphi + \xi_{m_2}^{(y)} \sin \theta \sin \varphi + \xi_{m_2}^{(z)} \cos \theta \right) \right\} \\ &= 2\pi \int_0^{\pi} d\theta \sin \theta e^{ik ||\mathbf{x}|| \cos \theta} \begin{bmatrix} \xi_{m_2}^{(x)} (1 - \frac{1}{2} \sin^2 \theta) \\ \xi_{m_2}^{(y)} (1 - \frac{1}{2} \sin^2 \theta) \\ \xi_{m_2}^{(z)} \sin^2 \theta \end{bmatrix} \equiv 2\pi \mathbf{I}(k, ||\mathbf{x}||). \end{aligned}$$

The integrals over θ give

$$I^{(x,y)}(k, ||\mathbf{x}||) = i \frac{\xi_{m_2}^{(x,y)}}{k ||\mathbf{x}||} \left[(e^{-ik ||\mathbf{x}||} - e^{ik ||\mathbf{x}||}) - \frac{i}{k ||\mathbf{x}||} (e^{-ik ||\mathbf{x}||} + e^{ik ||\mathbf{x}||}) - \frac{1}{(k ||\mathbf{x}||)^2} (e^{-ik ||\mathbf{x}||} - e^{ik ||\mathbf{x}||}) \right], \quad (19)$$

$$I^{(z)}(k, ||\mathbf{x}||) = -2i \frac{\xi_{m_2}^{(z)}}{k ||\mathbf{x}||} \left[-\frac{i}{k ||\mathbf{x}||} (e^{-ik ||\mathbf{x}||} + e^{ik ||\mathbf{x}||}) - \frac{1}{(k ||\mathbf{x}||)^2} (e^{-ik ||\mathbf{x}||} - e^{ik ||\mathbf{x}||}) \right]. \quad (20)$$

As we can see, the photon wave function contains contributions proportional to $1/|\mathbf{x}|$, $1/|\mathbf{x}|^2$, and $1/|\mathbf{x}|^3$, which are respectively known as the far-field, midfield, and near-field contributions. We then have

$$\psi_{\perp}(\mathbf{x}, t) = -i \frac{2^{\frac{7}{2}} \hbar e}{3^4 \epsilon_0 m_e a_0} \int_0^{+\infty} \frac{dk}{(2\pi)^2} k^2 \frac{e^{-ickt}}{\left[1 + \left(\frac{k}{k_X}\right)^2\right]^2} \mathbf{I}(k, |\mathbf{x}|) \int_0^t dt' c_e(t') e^{i(ck - \omega_0)t'}. \quad (21)$$

In most of what follows we will use the Wigner-Weisskopf approximation of exponential decay. We shall then have

$$c_e(t) = e^{-i\omega_{LS}t} e^{-\frac{1}{2}\Gamma t}, \quad (22)$$

where ω_{LS} is the partial Lamb shift [21] of the excited $2P$ level due to the $1S$ level and Γ is the decay rate. This yields

$$\int_0^t dt' c_e(t') e^{i(ck - \omega_0)t'} = \int_0^t dt' e^{i(ck - (\omega_0 + \omega_{LS}))t'} e^{-\frac{1}{2}\Gamma t'} = \left[\frac{e^{i(ck - (\omega_0 + \omega_{LS}))t'} e^{-\frac{1}{2}\Gamma t'}}{i(ck - (\omega_0 + \omega_{LS})) - \frac{1}{2}\Gamma} \right]_0^t = i \frac{1 - e^{i(ck - (\omega_0 + \omega_{LS}))t} e^{-\frac{1}{2}\Gamma t}}{ck - (\omega_0 + \omega_{LS}) + \frac{i}{2}\Gamma}. \quad (23)$$

We introduce the space-saving notation,

$$\Omega_0 \equiv \omega_0 + \omega_{LS} - \frac{i}{2}\Gamma. \quad (24)$$

We can then write the contributions to the far field, midfield, and near field to this photon wave function:

$$\psi_{\perp(\text{far})}^{(x,y)} = i \frac{2^{\frac{7}{2}} \hbar e}{3^4 \epsilon_0 m_e a_0} \frac{\xi_{m_2}^{(x,y)}}{|\mathbf{x}|} \int_0^{+\infty} \frac{dk}{(2\pi)^2} k \frac{e^{-i\Omega_0 t}}{\left[1 + \left(\frac{k}{k_X}\right)^2\right]^2} (e^{-ik|\mathbf{x}|} - e^{ik|\mathbf{x}|}) \frac{1 - e^{-i(ck - \Omega_0)t}}{ck - \Omega_0}, \quad (25a)$$

$$\psi_{\perp(\text{mid})}^{(x,y)} = \frac{2^{\frac{7}{2}} \hbar e}{3^4 \epsilon_0 m_e a_0} \frac{\xi_{m_2}^{(x,y)}}{|\mathbf{x}|^2} \int_0^{+\infty} \frac{dk}{(2\pi)^2} \frac{e^{-i\Omega_0 t}}{\left[1 + \left(\frac{k}{k_X}\right)^2\right]^2} (e^{-ik|\mathbf{x}|} + e^{ik|\mathbf{x}|}) \frac{1 - e^{-i(ck - \Omega_0)t}}{ck - \Omega_0}, \quad (25b)$$

$$\psi_{\perp(\text{near})}^{(x,y)} = -i \frac{2^{\frac{7}{2}} \hbar e}{3^4 \epsilon_0 m_e a_0} \frac{\xi_{m_2}^{(x,y)}}{|\mathbf{x}|^3} \int_0^{+\infty} \frac{dk}{(2\pi)^2} \frac{1}{k} \frac{e^{-i\Omega_0 t}}{\left[1 + \left(\frac{k}{k_X}\right)^2\right]^2} (e^{-ik|\mathbf{x}|} - e^{ik|\mathbf{x}|}) \frac{1 - e^{-i(ck - \Omega_0)t}}{ck - \Omega_0}, \quad (25c)$$

$$\psi_{\perp(\text{far})}^{(z)} = 0, \quad (25d)$$

$$\psi_{\perp(\text{mid})}^{(z)} = -\frac{2^{\frac{9}{2}} \hbar e}{3^4 \epsilon_0 m_e a_0} \frac{\xi_{m_2}^{(z)}}{|\mathbf{x}|^2} \int_0^{+\infty} \frac{dk}{(2\pi)^2} \frac{e^{-i\Omega_0 t}}{\left[1 + \left(\frac{k}{k_X}\right)^2\right]^2} (e^{-ik|\mathbf{x}|} + e^{ik|\mathbf{x}|}) \frac{1 - e^{-i(ck - \Omega_0)t}}{ck - \Omega_0}, \quad (25e)$$

$$\psi_{\perp(\text{near})}^{(z)} = i \frac{2^{\frac{9}{2}} \hbar e}{3^4 \epsilon_0 m_e a_0} \frac{\xi_{m_2}^{(z)}}{|\mathbf{x}|^3} \int_0^{+\infty} \frac{dk}{(2\pi)^2} \frac{1}{k} \frac{e^{-i\Omega_0 t}}{\left[1 + \left(\frac{k}{k_X}\right)^2\right]^2} (e^{-ik|\mathbf{x}|} - e^{ik|\mathbf{x}|}) \frac{1 - e^{-i(ck - \Omega_0)t}}{ck - \Omega_0}. \quad (25f)$$

B. General method

We write

$$\begin{aligned} H_n^{(\pm)}(|\mathbf{x}|, t) &\equiv \int_0^{+\infty} dk \frac{k^{2-n}}{\left[1 + \left(\frac{k}{k_X}\right)^2\right]^2} e^{\pm ik|\mathbf{x}|} \frac{1 - e^{-i(ck - \omega_0)t}}{ck - \omega_0} \\ &\equiv \int_0^{+\infty} dk f_n(k) e^{\pm ik|\mathbf{x}|}. \end{aligned} \quad (26)$$

It is a general result of distribution theory [22] that

$$\begin{aligned} H_n^{(\pm)}(|\mathbf{x}|, t) &= \frac{1}{2} \left[\left(\delta(\cdot) - \frac{i}{\pi} \text{P} \frac{1}{\cdot} \right) * \bar{f}_n(\cdot, t) \right] (\mp |\mathbf{x}|) \\ &\equiv \frac{1}{2} \bar{f}_n(\mp |\mathbf{x}|, t) - \frac{i}{2\pi} \lim_{\epsilon \rightarrow 0^+} \left[\int_{-\infty}^{-\epsilon} + \int_{\epsilon}^{+\infty} \right] \\ &\quad \times \frac{d\sigma}{\mp |\mathbf{x}| - \sigma} \bar{f}_n(\sigma, t), \end{aligned} \quad (27)$$

where P stands for the principal value, the asterisk denotes the convolution product, and

$$\bar{f}_n(|\mathbf{x}|, t) = \int_{-\infty}^{+\infty} dk f_n(k, t) e^{-ikx}. \quad (28)$$

In what follows we will endeavor to compute the $H_n^{(\pm)}$ integrals, first by making use of several approximations in order to obtain a causal result, and thereafter progressively waiving these approximations.

IV. CAUSALITY IN THE STANDARD TREATMENT

Here we use the following standard [1,11] approximations used to establish the causality of the wave function of the emitted photon: the Wigner-Weisskopf exponential decay, the usual $\hat{\mathbf{E}} \cdot \hat{\mathbf{x}}$ coupling between the field and the atom instead of the minimal $\hat{\mathbf{A}} \cdot \hat{\mathbf{p}}$ coupling, the dipole approximation, and the approximation which consists, as we will see, in extending the range of electromagnetic frequencies to the negative real semiaxis.

We switch (only in the present section) from the minimal $\hat{\mathbf{A}} \cdot \hat{\mathbf{p}}$ to the usual $\hat{\mathbf{E}} \cdot \hat{\mathbf{x}}$ coupling. In the dipole approximation, which, for the $\hat{\mathbf{A}} \cdot \hat{\mathbf{p}}$ coupling, consists [23] in forgetting about the $[1 + (k/k_X)^2]^2$ denominator in Eq. (21), this substitution results [12,15] in the multiplication of the interaction matrix

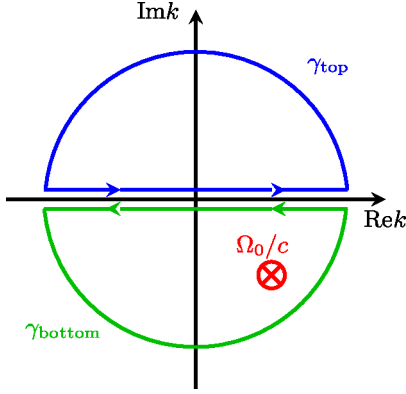


FIG. 1. Jordan loops in the complex k plane used to compute the integrals (30). The (isolated) simple pole Ω_0/c of the integrands is represented by a red circled cross.

element by ck/ω_0 . Plugging this in Eq. (21), we have

$$\psi_{\perp}(\mathbf{x}, t) = -\frac{2^{\frac{7}{2}}}{3^4} \frac{\hbar e c}{\epsilon_0 m_e a_0 \omega_0} \int_0^{+\infty} \frac{dk}{(2\pi)^2} k^3 e^{-i\Omega_0 t} \times \mathbf{I}(k, |\mathbf{x}|) \frac{1 - e^{-i(ck - \Omega_0)t}}{ck - \Omega_0}. \quad (29)$$

$$\psi_{\perp}(\mathbf{x}, t) = \frac{2^{\frac{5}{2}}}{3^4 \pi} \frac{\hbar e}{\epsilon_0 m_e a_0 \omega_0} \theta(ct - |\mathbf{x}|) \left(\frac{\Omega_0}{c}\right)^3 \left[\begin{array}{l} \xi^{(x,y)} \left(\frac{1}{\frac{\Omega_0}{c}|\mathbf{x}|} + \frac{i}{\left(\frac{\Omega_0}{c}|\mathbf{x}| \right)^2} - \frac{1}{\left(\frac{\Omega_0}{c}|\mathbf{x}| \right)^3} \right) \\ - 2\xi^{(z)} \left(\frac{i}{\left(\frac{\Omega_0}{c}|\mathbf{x}| \right)^2} - \frac{1}{\left(\frac{\Omega_0}{c}|\mathbf{x}| \right)^3} \right) \end{array} \right] e^{i\frac{\Omega_0}{c}(|\mathbf{x}| - ct)}. \quad (32)$$

V. MINIMAL COUPLING IN THE DIPOLE APPROXIMATION

A. Causality in the mid- and far-field regions

We now return to what we regard as the more correct coupling: the minimal $\hat{\mathbf{A}} \cdot \hat{\mathbf{p}}$ coupling. We still work in the dipole approximation and in the Wigner-Weisskopf approximation. We shall first extend the range of integration to the negative real semiaxis as was done in the previous section IV. This yields

$$\psi_{\perp}(\mathbf{x}, t) = -\frac{2^{\frac{7}{2}}}{3^4} \frac{\hbar e}{\epsilon_0 m_e a_0} \int_{-\infty}^{+\infty} \frac{dk}{(2\pi)^2} k^2 e^{-i\Omega_0 t} \times \mathbf{I}(k, |\mathbf{x}|) \frac{1 - e^{-i(ck - \Omega_0)t}}{ck - \Omega_0}. \quad (33)$$

We find ourselves computing the following Fourier transforms:

$$\begin{aligned} \bar{f}_{n(\text{dip})}(\mp|\mathbf{x}|, t) &\equiv \int_{-\infty}^{+\infty} dk k^{2-n} e^{\pm ik|\mathbf{x}|} \frac{1 - e^{-i(ck - \Omega_0)t}}{ck - \Omega_0} \\ &\equiv \int_{-\infty}^{+\infty} dk f_{n(\text{dip})}(k) e^{\pm ik|\mathbf{x}|}. \end{aligned} \quad (34)$$

Here the dip subscript stands for ‘‘dipole’’ as we use the dipole-approximated minimal $\hat{\mathbf{A}} \cdot \hat{\mathbf{p}}$ coupling. We use Cauchy’s residue theorem (see Fig. 2). Taking into account the fact that t and $|\mathbf{x}|$ are positive quantities, we find, for $n \in \{1, 2\}$,

The usual trick [1,2,11] is then to extend the range of integration from the positive real semiaxis to the whole real axis, and we find ourselves computing integrals of the type

$$H_{n(\text{std})}^{(\pm)}(|\mathbf{x}|, t) \equiv \int_{-\infty}^{+\infty} dk k^{3-n} e^{\pm ik|\mathbf{x}|} \frac{1 - e^{-i(ck - \Omega_0)t}}{ck - \Omega_0}, \quad (30)$$

with $n \in \{1, 2, 3\}$, and where the label $+(-)$ is assigned to outgoing (ingoing) radial waves. Here the std subscript stands for ‘‘standard’’ as we follow the lines of the standard treatment [1,11] of the problem. For this we use Cauchy’s residue theorem (see Fig. 1). Taking into account the fact that t and $|\mathbf{x}|$ are positive quantities, we find (for more details, see the similar treatment of Sec. V A)

$$\begin{aligned} H_{n(\text{std})}^{(+)}(|\mathbf{x}|, t) &= 2\frac{i\pi}{c} \theta(ct - |\mathbf{x}|) \left(\frac{\Omega_0}{c}\right)^{3-n} e^{i\frac{\Omega_0}{c}|\mathbf{x}|}, \\ H_{n(\text{std})}^{(-)}(|\mathbf{x}|, t) &= 0. \end{aligned} \quad (31)$$

This means that contributions from ingoing waves are zero, as found for instance in Ref. [11]. As made clear by the Heaviside step, this result is explicitly causal. We finally have

whence

$$\bar{f}_{n(\text{dip})}(u, t) = \left(\frac{\Omega_0}{c}\right)^{2-n} e^{-i\frac{\Omega_0}{c}u} [-\theta(u) + \theta(u + ct)], \quad (35a)$$

$$\bar{f}_{n(\text{dip})}(|\mathbf{x}|, t) = 0, \quad (35b)$$

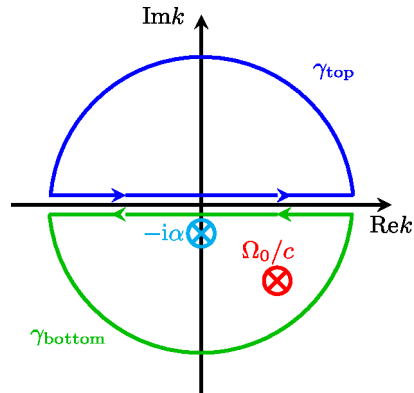


FIG. 2. Jordan loops in the complex k plane used to compute the integrals (34). The (isolated) simple poles Ω_0/c and $-i\alpha$ of the integrands are represented by a red and a cyan circled cross, respectively.

and

$$\bar{f}_{n(\text{dip})}(-|\mathbf{x}|, t) = 2i\pi \left(\frac{\Omega_0}{c}\right)^{2-n} e^{i\frac{\Omega_0}{c}|\mathbf{x}|} \theta(-|\mathbf{x}| + ct), \quad (35c)$$

from which we conclude

$$\begin{aligned} \bar{f}_{n(\text{dip})}(-|\mathbf{x}|, t) &\mp \bar{f}_{n(\text{dip})}(|\mathbf{x}|, t) \\ &= 2i\pi \left(\frac{\Omega_0}{c}\right)^{2-n} e^{i\frac{\Omega_0}{c}|\mathbf{x}|} \theta(-|\mathbf{x}| + ct), \end{aligned} \quad (35d)$$

which is transparently causal. Notice from (35b) that the contributions from ingoing waves are identically zero here, as they were in the standard treatment of Sec. IV. As far as we know, similar calculations [1,3,5,11] of the outgoing field have mostly been carried out in the Power-Zineau-Woolley picture [12] of quantum electrodynamics where the interaction Hamiltonian is of the usual $\hat{\mathbf{E}} \cdot \hat{\mathbf{x}}$ form. In this case one retrieves a causal result, as was done in Sec. IV, even for the near field; this is no longer true if one considers the minimal coupling. The $n = 3$ case which corresponds, as can be seen from (19), to the near-field part of the emitted photon wave function, is not further considered here. In the present manuscript we will focus on the mid- and far-field contributions to the electric field, and shall return to the delicate question of the near field in an upcoming manuscript [24].

B. Hegerfeldt theorem for the minimal coupling in the dipole approximation

We now waive the approximation which consists in extending the range of integration to the negative real semiaxis as was done in the previous Secs. IV and V A. This yields

$$\begin{aligned} \psi_{\perp}(\mathbf{x}, t) &= -\frac{2^{\frac{7}{2}}}{3^4} \frac{\hbar e}{\epsilon_0 m_e a_0} \int_0^{+\infty} \frac{dk}{(2\pi)^2} k^2 e^{-i\Omega_0 t} \\ &\times \mathbf{I}(k, |\mathbf{x}|) \frac{1 - e^{-i(ck - \Omega_0)t}}{ck - \Omega_0} \end{aligned} \quad (36)$$

and we find ourselves computing integrals of the type

$$\begin{aligned} H_{n(\text{dip})}^{(\pm)}(|\mathbf{x}|, t) &\equiv \int_0^{+\infty} dk k^{2-n} e^{\pm ik|\mathbf{x}|} \frac{1 - e^{-i(ck - \Omega_0)t}}{ck - \Omega_0} \\ &\equiv \int_{-\infty}^{+\infty} dk \theta(k) f_{n(\text{dip})}(k) e^{\pm ik|\mathbf{x}|}, \end{aligned} \quad (37)$$

with $n \in \{1, 2\}$. With (27) in mind we can use the Fourier transform $\bar{f}_{n(\text{dip})}$ of $f_{n(\text{dip})}$ computed in Sec. V A. Since we did not extend the range of integration to the whole real axis, we will not retrieve a causal propagation, as first noted by Shirokov [2]. Note that this is true regardless of the choice for the coupling: Fermi's proof of causality used the usual $\hat{\mathbf{E}} \cdot \hat{\mathbf{x}}$ coupling, and included, as an approximation necessary to causality, the extension of the range of integration to the whole real axis. This is an illustration of the Hegerfeldt theorem [4], which states that noncausalities will always arise for Hamiltonians bounded by below. The relevant Hamiltonian here for the Hegerfeldt theorem is the Hamiltonian \hat{H}_R (1) of the free field, which has \mathbb{R}_+ as its spectrum and is hence bounded.

We now focus on the Hegerfeldt noncausality. To investigate this particular point, we compute the convolutions of (35d)

with the principal value as prescribed by (27). In the mid- and far field we get ($n \in \{1, 2\}$)

$$\begin{aligned} C_{n(\text{dip})}(|\mathbf{x}|, t) &\equiv -\frac{i}{2\pi} \left[\mathcal{P} \frac{1}{\cdot} * \bar{f}_{n(\text{dip})}(\cdot, t) \right] (|\mathbf{x}|) \\ &= e^{-i\frac{\Omega_0}{c}|\mathbf{x}|} \left(\frac{\Omega_0}{c}\right)^{2-n} \left[-\text{Ei}\left(i\frac{\Omega_0}{c}|\mathbf{x}| \right) \right. \\ &\quad \left. + \text{Ei}\left(i\frac{\Omega_0}{c}(|\mathbf{x}| + ct) \right) \right]. \end{aligned} \quad (38)$$

Here Ei stands for the exponential integral [25]

$$\text{Ei}(x) \equiv -\int_{-x}^{+\infty} du \frac{e^{-u}}{u}. \quad (39)$$

Note that to deduce $\bar{f}_{n(\text{dip})}$, as given by (35b), from (27) and (34), we made unwarranted use of Jordan's lemma: the integral of $f_{n(\text{dip})}$ over the semicircle in the integration path γ_{top} (see Fig. 2) is not zero for $n = 1$ in the limit of large semicircle radius. On the contrary, this integral diverges in that limit [26]. It is thus clear that the dipole approximation forbids a clear, consistent treatment of the problem at hand (unless a cutoff is introduced around the frequency $\omega_X = (3c)/(2a_0)$ as explained in Refs. [15,23]; however, if a cutoff is introduced we cannot avoid Hegerfeldt-type noncausalities). In the next Sec. VI we do away with the dipole approximation. Nevertheless, we will see that very similar terms to those obtained here in the framework of the dipole approximation arise. Since the expressions obtained are much more involved in the next Sec. VI, we study the less complicated results of the present section in some detail, and this knowledge will come in handy for later. Namely, taking the $k_X \rightarrow +\infty$ limit of the results of Sec. VI yields the results in the dipole approximation. This confirms that the exact coupling provides the correct regularization for the dipole approximation (see [15,23]).

We plot in Fig. 3 the square moduli of the causal (or pole) (35d) and noncausal (or principal value) (38) contributions to the far- and midfield parts of the emitted photon wave function.

Two noticeable patterns emerge as follows:

(i) Inside the light cone, we notice that the contributions to the far field ($n = 1$) from the pole term (35d) and from the principal value term (38) are almost indistinguishable, at least when $|\mathbf{x}| < c/\Omega_0$. This feature can be explained by simple asymptotic arguments: under the condition that we pick a space-time point reasonably "deep" within the light cone, we may make the approximation that $|\mathbf{x}|/(ct) \rightarrow 0$ so that from (38) and the asymptotic series [25]

$$\text{Ei}(u) \underset{u \rightarrow +\infty}{\sim} \frac{e^u}{u} \sum_{k=0}^{+\infty} \frac{k!}{u^k}, \quad (40)$$

we may write, with the extra help of the Taylor series for Ei(u) around $u = 0$,

$$C_{1(\text{dip})}(-|\mathbf{x}|, t) - C_{1(\text{dip})}(|\mathbf{x}|, t) \underset{\frac{\Omega_0}{c}|\mathbf{x}| \rightarrow 0}{\sim} i\pi \frac{\Omega_0}{c}, \quad (41)$$

in agreement with the asymptotic behavior of the causal part (35d) in the same $(\Omega_0/c)|\mathbf{x}| \ll 1$ limit. This good agreement is not reached for the midfield because the contributions from ingoing and outgoing waves are added instead of subtracted, as seen in Eq. (19).

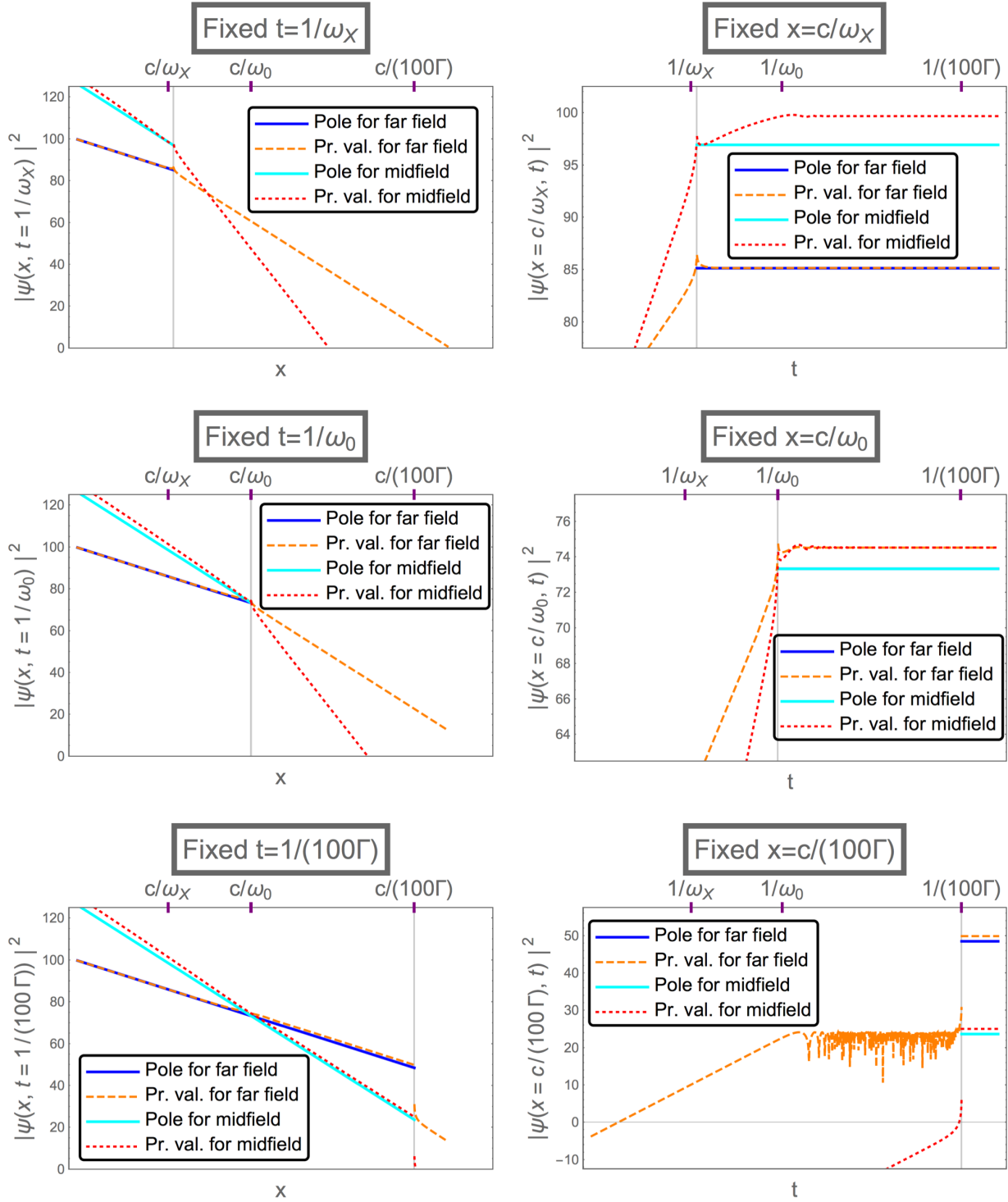


FIG. 3. Square moduli of the contributions to the far- ($n = 1$) and mid- ($n = 2$) fields from the poles as given by (35d) and from the principal value integrals as given by (38) as a function of distance from the nucleus, for fixed time in the left column, and as a function of time, for fixed distance in the right column. This is for the minimal $\hat{\mathbf{A}} \cdot \hat{\mathbf{p}}$ coupling in the dipole approximation (Sec. VB). Both axes are logarithmic on all figures. The boundary of the light cone is signaled by a vertical line. The reader will notice the noteworthy fact that, for fixed $x = c/\omega_0$, the contributions from the mid-field and far field are indistinguishable inside the light cone.

(ii) Outside the light cone (where the only contributions to the far and mid-field, obviously, come from the principal value integrals), we notice on the graphs that the ($n = 1$) far field decays not as $1/|\mathbf{x}|$ as expected, but as $1/|\mathbf{x}|^2$. As for the ($n = 2$) mid-field, it decays not as $1/|\mathbf{x}|^2$ as expected, but

as $1/|\mathbf{x}|^4$. Again, this can be explained by the asymptotic behavior [25] of the exponential integral function: under the condition that we pick a space-time point reasonably far away from the light cone, we may make the approximation that $|\mathbf{x}|/(ct) \rightarrow +\infty$ so that from (38) and (40) we may write the

asymptotic series,

$$C_{1(\text{dip})}(-|\mathbf{x}|, t) - C_{1(\text{dip})}(|\mathbf{x}|, t) \simeq -\frac{2i(-1 + e^{i\Omega_0 t})}{|\mathbf{x}|} \left(\text{for large } \frac{\Omega_0}{c} |\mathbf{x}| \right), \quad (42a)$$

$$C_{2(\text{dip})}(-|\mathbf{x}|, t) + C_{2(\text{dip})}(|\mathbf{x}|, t) \simeq \frac{2 + e^{i\Omega_0 t}(-2 + 2i\Omega_0 t)}{\left(\frac{\Omega_0}{c}\right)^2 |\mathbf{x}|^2} \quad (\text{i.d.}), \quad (42b)$$

This accounts for the spacewise-decay behavior described just above. The conclusion reached is interesting: outside the light cone, the far field decays more strongly than usual with increasing distance and mimics the usual behavior of the midfield ($1/|\mathbf{x}|^2$), while the midfield decays much more strongly than usual with increasing distance, so that its $1/|\mathbf{x}|^4$ decay is stronger than the usual $1/|\mathbf{x}|^3$ decay of the near field.

Both these points are noteworthy features of the Hegerfeldt-noncausal terms, which come from the fact that the integration is restricted to positive electromagnetic frequencies, as it should be. The first point confirms that the usual approximation consisting in extending the integration to the negative real semiaxis is fairly solid: inside the light cone, we see (Fig. 3) that the contribution from the (principal value) noncausal terms (38) just about equals that of the (pole) causal terms (35d), which means that the result yielded by extending the range of integration would be sensible. As for what happens outside the light cone, we not only pointed to the well-known fact that taking the absence of negative frequencies into account yields a nonzero result, but we noticed the interesting fact that the field decays more strongly with increasing distance than would be naively inferred from the usual behavior of the mid- and far-field contributions to the emitted electric field. Keep in mind that the noncausal contributions to the emitted field are small, as seen on Fig. 3 (remember that the axes are logarithmic).

VI. EXACT TREATMENT FOR THE MINIMAL COUPLING

A. Derivation

We now switch to a fully rigorous treatment of the problem. We use the minimal $\hat{\mathbf{A}} \cdot \hat{\mathbf{p}}$ form of the atom-field coupling. We no longer work in the dipole approximation, but shall instead use the exact interaction matrix element (6). We also no longer perform the Wigner-Weisskopf approximation but use perturbation theory at short times [27]. Finally, we do not extend the range of integration to the negative real semiaxis as was done in Secs. IV and V A. In a time-dependent perturbative treatment of the present problem, we approximate (21) to first order in time, which consists [23] in considering that $c_e(t) = 1$, so that the photon wave function is approximated by

$$\psi_{\perp}(\mathbf{x}, t) = -\frac{2^{\frac{7}{2}} \hbar e}{3^4 \epsilon_0 m_e a_0} \int_0^{+\infty} \frac{dk}{(2\pi)^2} \frac{k^2}{\left[1 + \left(\frac{k}{k_x}\right)^2\right]^2} \times e^{-i\omega_0 t} \mathbf{I}(k, |\mathbf{x}|) \frac{1 - e^{-i(ck - \omega_0)t}}{ck - \omega_0}. \quad (43)$$

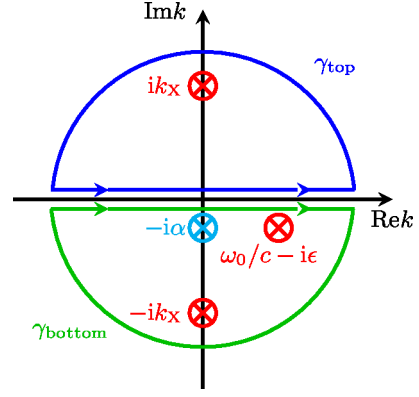


FIG. 4. Jordan loops in the complex k plane used to compute the Fourier transform (47). The (isolated) poles $\omega_0/c - i\epsilon$ and $\pm ik_x$ are represented by red circled crosses, while the (isolated) simple pole $-i\alpha$ is represented by a cyan circled cross.

We find ourselves computing integrals of the type

$$H_n^{(\pm)}(|\mathbf{x}|, t) \equiv \int_0^{+\infty} dk \frac{k^{2-n}}{\left[1 + \left(\frac{k}{k_x}\right)^2\right]^2} e^{\pm ik|\mathbf{x}|} \frac{1 - e^{-i(ck - \omega_0)t}}{ck - \omega_0}, \quad (44)$$

with $n \in \{1, 2, 3\}$. The integrand is similar to that in Eq. (34), but features two extra poles at $k = \pm ik_x$, and its ‘‘Wigner-Weisskopf’’ pole at $k = \omega_0/c$ sits on the real axis. Since the latter is only an artificial singularity, we can shift it to the lower half plane as seen on Fig. 4. For $n = 3$ we see that the integrand in Eq. (44) has a pole at $k = 0$. We will not dwell on this near-field case in what follows, though.

We can [28] rewrite (44) as

$$\begin{aligned} H_n^{(\pm)}(|\mathbf{x}|, t) & \equiv \int_{-\infty}^{+\infty} dk \frac{\theta(k)(k + i\alpha)^{2-n}}{\left[1 + \left(\frac{k}{k_x}\right)^2\right]^2} e^{\pm ik|\mathbf{x}|} \frac{1 - e^{-i(ck - \omega_0)t}}{ck - (\omega_0 - i\epsilon)} \\ & \equiv \int_{-\infty}^{+\infty} dk \theta(k) f_n(k, t) e^{\pm ik|\mathbf{x}|} \\ & \equiv \int_{-\infty}^{+\infty} dk \theta(k) (g_n(k) - h_n(k, t)) e^{\pm ik|\mathbf{x}|}, \end{aligned} \quad (45)$$

where it is implied that the limit $\alpha \rightarrow 0^+$, $\epsilon \rightarrow 0^+$ should be taken outside the integral. Here the functions g_n and h_n read

$$g_n(k) \equiv \frac{(k + i\alpha)^{2-n}}{\left[1 + \left(\frac{k}{k_x}\right)^2\right]^2} \frac{1}{ck - (\omega_0 - i\epsilon)}, \quad (46a)$$

$$h_n(k, t) \equiv \frac{(k + i\alpha)^{2-n}}{\left[1 + \left(\frac{k}{k_x}\right)^2\right]^2} \frac{e^{-i(ck - \omega_0)t}}{ck - (\omega_0 - i\epsilon)}. \quad (46b)$$

Once again we use (27) and hence need to compute the Fourier transform

$$\bar{f}_n(|\mathbf{x}|, t) = \int_{-\infty}^{+\infty} dk f_n(k, t) e^{-ikx} \quad (47)$$

of f_n . We use Cauchy’s residue theorem. We know from (44) that f_n has a first order pole at $\omega_0/c - i\epsilon$ and two second order poles at $\pm ik_x$, pictured on Fig. 4. From (45) and (47) we see

that we have to close the integration path (Jordan loop) in the lower half of the complex plane for $|\mathbf{x}| > 0$ and $|\mathbf{x}| + ct > 0$

for g_n and h_n , respectively, and in the upper half of the plane for $|\mathbf{x}| < 0$ or $|\mathbf{x}| + ct < 0$ for g_n and h_n , respectively.

It can be checked that the residues of $g_n(\omega)e^{-ikx}$ and $h_n(\omega)e^{-ikx}$ read

$$\text{Res}\left[g_n(\cdot)e^{-i\cdot|\mathbf{x}|}, \frac{\omega_0}{c} - i\epsilon\right] \xrightarrow{\epsilon \rightarrow 0^+} e^{-i\frac{\omega_0}{c}|\mathbf{x}|} G_0^{(n)}, \tag{48a}$$

$$\text{Res}[g_n(\cdot)e^{-i\cdot|\mathbf{x}|}, ik_X] \xrightarrow{\epsilon \rightarrow 0^+} e^{k_X|\mathbf{x}|} [\gamma_0^{+(n)} + \gamma_1^{+(n)} |\mathbf{x}|], \tag{48b}$$

$$\text{Res}[g_n(\cdot)e^{-i\cdot|\mathbf{x}|}, -ik_X] \xrightarrow{\epsilon \rightarrow 0^+} e^{-k_X|\mathbf{x}|} [\gamma_0^{-(n)} + \gamma_1^{-(n)} |\mathbf{x}|] \tag{48c}$$

and

$$\text{Res}\left[h_n(\cdot, t)e^{-i\cdot|\mathbf{x}|}, \frac{\omega_0}{c} - i\epsilon\right] \xrightarrow{\epsilon \rightarrow 0^+} e^{-i\frac{\omega_0}{c}|\mathbf{x}|} G_0^{(n)}, \tag{49a}$$

$$\text{Res}[h_n(\cdot, t)e^{-i\cdot|\mathbf{x}|}, ik_X] \xrightarrow{\epsilon \rightarrow 0^+} e^{k_X|\mathbf{x}|} [\gamma_0^{+(n)} + \gamma_1^{+(n)} (|\mathbf{x}| + ct)], \tag{49b}$$

$$\text{Res}[h_n(\cdot, t)e^{-i\cdot|\mathbf{x}|}, -ik_X] \xrightarrow{\epsilon \rightarrow 0^+} e^{-k_X|\mathbf{x}|} [\gamma_0^{-(n)} + \gamma_1^{-(n)} (|\mathbf{x}| + ct)], \tag{49c}$$

where the $G_0^{(n)}$ and $\gamma_i^{\pm(n)}$ depend on n , as suggested by the notation. One can see that

$$\gamma_0^{+(n)} = \gamma_0^{-*(n)} \equiv \gamma_0^{(n)}, \quad \gamma_1^{+(n)} = -\gamma_1^{-*(n)} \equiv \gamma_1^{(n)}.$$

We give

$$G_0^{(n)} = \frac{\left(\frac{\omega_0}{c}\right)^{2-n} (ck_X)^4}{(\omega_0^2 + c^2k_X^2)^2}, \tag{50a}$$

$$\gamma_0^{(n)} = \frac{ck_X (ik_X)^{2-n} [-i(-3+n)\omega_0 - (n-2)ck_X]}{4(i\omega_0 + ck_X)^2}, \tag{50b}$$

$$\gamma_1^{(n)} = \frac{ck_X^2 (ik_X)^{2-n}}{4(i\omega_0 + ck_X)}. \tag{50c}$$

The Fourier transform (47) is thus given for $n \in \{1, 2\}$ by

$$\begin{aligned} \frac{\bar{f}_n(|\mathbf{x}|, t)}{2i\pi} &= -\theta(|\mathbf{x}|) [e^{-k_X|\mathbf{x}|} (\gamma_0^{*(n)} - \gamma_1^{*(n)} |\mathbf{x}|) + e^{-i\frac{\omega_0}{c}|\mathbf{x}|} G_0^{(n)}] + \theta(-|\mathbf{x}|) [e^{-k_X|\mathbf{x}|} (\gamma_0^{(n)} + \gamma_1^{(n)} |\mathbf{x}|)] \\ &+ \theta(|\mathbf{x}| + ct) [e^{i\omega_0 t} e^{-k_X(|\mathbf{x}|+ct)} (\gamma_0^{*(n)} - \gamma_1^{*(n)} (|\mathbf{x}| + ct)) + e^{-i\frac{\omega_0}{c}|\mathbf{x}|} G_0^{(n)}] \\ &- \theta(-(|\mathbf{x}| + ct)) [e^{i\omega_0 t} e^{k_X(|\mathbf{x}|+ct)} (\gamma_0^{(n)} + \gamma_1^{(n)} (|\mathbf{x}| + ct))]. \end{aligned} \tag{51}$$

We can then compute the convolution—which we call $C_n(|\mathbf{x}|, t)$ —with the principal value as prescribed by (27). It yields, still for $n \in \{1, 2\}$ (the $n = 3$ contribution will be discussed in Ref. [28]),

$$\begin{aligned} C_n(|\mathbf{x}|, t) &\equiv -\frac{i}{2\pi} \left[\text{P} \frac{1}{\cdot} * \bar{f}_n(\cdot, t) \right] (|\mathbf{x}|) \\ &= e^{-k_X|\mathbf{x}|} \left[(\gamma_0^{*(n)} - \gamma_1^{*(n)} |\mathbf{x}|) [-\text{Ei}(k_X|\mathbf{x}|) + e^{(i\omega_0 - ck_X)t} \text{Ei}(k_X(|\mathbf{x}| + ct))] \right. \\ &+ \frac{\gamma_1^{*(n)}}{k_X} (-e^{k_X|\mathbf{x}|} + e^{(i\omega_0 - ck_X)t} e^{k_X(|\mathbf{x}|+ct)}) - c\gamma_1^{*(n)} t e^{(i\omega_0 - ck_X)t} \text{Ei}(k_X(|\mathbf{x}| + ct)) \left. \right] \\ &+ e^{k_X|\mathbf{x}|} \left[(\gamma_0^{(n)} + \gamma_1^{(n)} |\mathbf{x}|) [-\text{Ei}(-k_X|\mathbf{x}|) + e^{(i\omega_0 + ck_X)t} \text{Ei}(k_X(-|\mathbf{x}| - ct))] \right. \\ &+ \frac{\gamma_1^{(n)}}{k_X} (-e^{-k_X|\mathbf{x}|} + e^{(i\omega_0 + ck_X)t} e^{k_X(-|\mathbf{x}| - ct)}) + c\gamma_1^{(n)} t e^{(i\omega_0 + ck_X)t} \text{Ei}(k_X(-|\mathbf{x}| - ct)) \left. \right] \\ &+ e^{-i\frac{\omega_0}{c}|\mathbf{x}|} G_0^{(n)} \left[-\text{Ei}\left(i\frac{\omega_0}{c}|\mathbf{x}| \right) + \text{Ei}\left(i\frac{\omega_0}{c}(|\mathbf{x}| + ct) \right) \right]. \end{aligned} \tag{52}$$

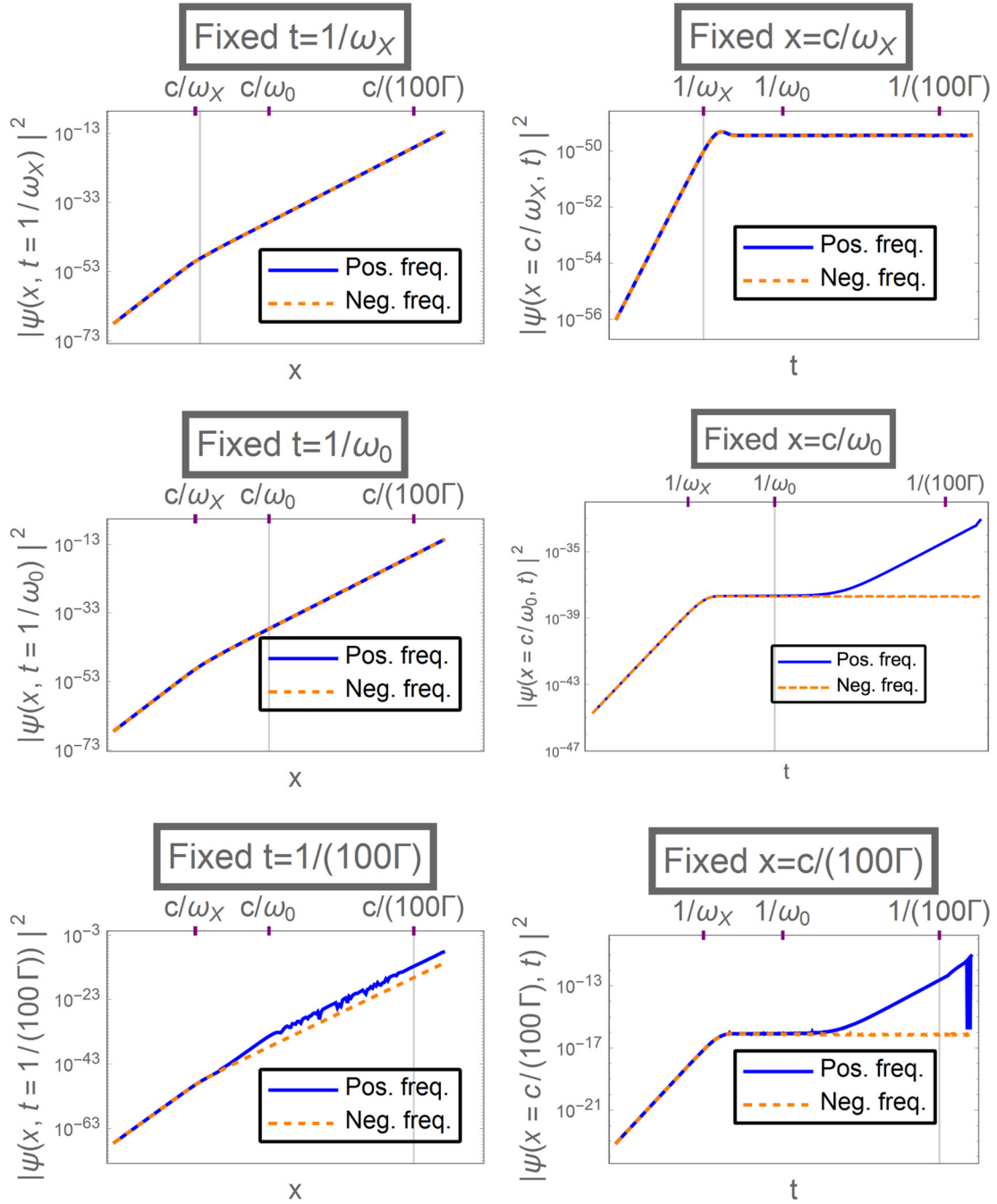


FIG. 5. Square moduli of the contributions from the positive (solid blue) and (nonexistent, but included in the usual approximation which yields a causal result; see Sec. V A) negative (dashed orange) frequencies to the emitted field, as a function of distance for fixed time in the left column, and as a function of time, for fixed distance in the right column. This is for the exact (multipolar) minimal $\hat{\mathbf{A}} \cdot \hat{\mathbf{p}}$ coupling, and all contributions from the near, mid-, and far field are included. Both axes are logarithmic on all figures. The boundary of the light cone is signaled by a vertical line. Notice that it is only at sufficiently large distances and long times that the unphysical contribution from the negative frequencies becomes negligible.

Keeping in mind that $\|\mathbf{x}\|$ and t are both positive we compute, for $n \in \{1, 2\}$

$$\begin{aligned}
 \bar{f}_n(-\|\mathbf{x}\|, t) \mp \bar{f}_n(\|\mathbf{x}\|, t) = 2i\pi \{ & G_0^{(n)} \theta(-\|\mathbf{x}\| + ct) e^{i\frac{\omega_0}{c}\|\mathbf{x}\|} + \theta(-\|\mathbf{x}\| + ct) e^{i\omega_0 t} [e^{-k_x(ct-\|\mathbf{x}\|)} (\gamma_0^{*(n)} + \gamma_1^{*(n)}(\|\mathbf{x}\| - ct)) \\
 & + e^{k_x(ct-\|\mathbf{x}\|)} (\gamma_0^{(n)} - \gamma_1^{(n)}(\|\mathbf{x}\| - ct))] + e^{-k_x\|\mathbf{x}\|} [(\gamma_0^{(n)} \mp \gamma_0^{*(n)}) - (\gamma_1^{(n)} \mp \gamma_1^{*(n)})\|\mathbf{x}\|] \\
 & - e^{i\omega_0 t} [\mp e^{-k_x(ct+\|\mathbf{x}\|)} (\gamma_0^{*(n)} - \gamma_1^{*(n)}(\|\mathbf{x}\| + ct)) + e^{k_x(ct-\|\mathbf{x}\|)} (\gamma_0^{(n)} - \gamma_1^{(n)}(\|\mathbf{x}\| - ct))] \}. \quad (53)
 \end{aligned}$$

The quantities $C_n(-||\mathbf{x}||,t) \mp C_n(||\mathbf{x}||,t)$ are not illuminating enough to warrant their explicit writing out here, but their expression follows immediately from (52). Also, note that (27) can be rewritten,

$$H_n^{(\pm)}(||\mathbf{x}||,t) = \frac{1}{2} \bar{f}_n(\mp ||\mathbf{x}||,t) - C_n(\mp ||\mathbf{x}||,t), \tag{54}$$

and the photon wave function is given, according to (19), (43), and (44), by

$$\psi_{\perp}(\mathbf{x},t) = -i \frac{2^{\frac{7}{2}}}{3^4} \frac{\hbar e}{\epsilon_0 m_e a_0} \frac{e^{-i\omega_0 t}}{(2\pi)^2} \times \left(\begin{array}{l} \frac{\xi_{m_2}^{(x,y)}}{||\mathbf{x}||} \left[[H_1^{(-)} - H_1^{(+)}](||\mathbf{x}||,t) - \frac{i}{||\mathbf{x}||} [H_2^{(-)} + H_2^{(+)}](||\mathbf{x}||,t) - \frac{1}{||\mathbf{x}||^2} [H_3^{(-)} - H_3^{(+)}](||\mathbf{x}||,t) \right] \\ 2 \frac{\xi_{m_2}^{(z)}}{||\mathbf{x}||} \left[\frac{i}{||\mathbf{x}||} [H_2^{(-)} + H_2^{(+)}](||\mathbf{x}||,t) + \frac{1}{||\mathbf{x}||^2} [H_3^{(-)} - H_3^{(+)}](||\mathbf{x}||,t) \right] \end{array} \right), \tag{55}$$

where it is of course understood that the values of all functions $H_i^{(\pm)}$ are taken at $(||\mathbf{x}||,t)$. Remember that $\xi_{m_2}^{(x,y)}$ are the components of ξ_{m_2} in the plane perpendicular to \mathbf{x} , while $\xi_{m_2}^{(z)}$ is the component of ξ_{m_2} in the direction of \mathbf{x} .

B. Discussion

According to (51) and (52) our final result given by (54) and (55) is evidently noncausal. We identify two sources of noncausality as follows:

(i) The first one is well known [2,4] and is due to the fact that, in order to compute the photon wave function, we integrated over the physical frequencies of the electromagnetic field, which are positive. Indeed, the spectrum of the electromagnetic field Hamiltonian is the positive real semiaxis and is thus bounded from below. In light of Hegerfeldt’s theorem, it is then not surprising to observe that our result is noncausal. More precisely, the theorem teaches that the convolution contribution (52), which would not be featured if the integration was carried out over the whole real axis, necessarily introduces a noncausality in Eq. (54). This feature has already been studied in Sec. VB, where the dipole approximation was performed, which changes little to the discussion and the results.

(ii) The second one is the uncertainty on the position of the electron. For instance, at $t = 0$, when the emission starts, the electron is in the $2P$ level, and its wave function is spread on a distance of order $2a_0$. In the light of this uncertainty, it is natural to expect a spacewise-exponentially decreasing tail in the emitted field, with characteristic size of order a_0 . And this is what we indeed obtain if we neglect the other sources of noncausality, namely if we integrate in Eq. (43) over both positive and negative frequencies; in other words, if we consider only expression Eq. (53), the result is still noncausal. In the previous sentence “noncausal” is understood to mean “not vanishing outside the light cone centered around $t = 0$ and the position $\mathbf{x} = \mathbf{0}$ of the hydrogen nucleus (proton).” Rather, the noncausal terms in (53) decay exponentially on a distance $3a_0/2$. These terms are nonvanishing outside the light cone centered around $t = 0$ and $\mathbf{x} = \mathbf{0}$, which we understand as being an illustration of the fact that the electron emits the photon from its own position, which is not fully determined and is only exponentially confined within distances of order a_0 around the nucleus, rather than from the position $\mathbf{x} = \mathbf{0}$

of the nucleus itself [29]. In Ref. [2], Shirokov very clearly hints at such exponentially decreasing tails outside the light cone. But among the works of his which are available to us (including [30]), none presents or even mentions the method he used to obtain this feature.

VII. ON THE APPROPRIATENESS OF INCLUDING NEGATIVE FREQUENCIES

The results presented in the previous sections regarding departure from causality are, of course, disturbing but maybe not exceedingly disturbing. Indeed, the weight of the wave function present outside the light cone is always small as can be seen for instance in Fig. 3. In another paper [31] we estimated that for a simpler but related problem, the weight of the negative frequencies after a time of the order of the lifetime is bounded by 10^{-10} , which could never explain for instance nonlocality effects in the manner of Bell characterized by violations of $1/\sqrt{2}$ (see footnote 3 in Ref. [31]). In order to systematize this study, we numerically evaluate the weight of the positive and negative frequency contributions to the wave function, in different regions of space-time. The results are shown on Fig. 5. They confirm the discussion of Sec. VIB: at large distances from the light cone the contributions of the “negative frequency modes” systematically vanish. It is only at a short distance that these virtual modes contribute in a significant manner to the wave function. Since we know from the previous sections that, up to an exponential tail in space, the contributions of positive and frequency modes add up to be exactly causal, we can safely conclude that the noncausality of the wave function of the photon emitted during the spontaneous decay process under study remains weak in all circumstances.

We see in Fig. 5 that, for intermediate and large distances from the atom, we retrieve two clearly defined time regimes, corresponding to the short-time Zeno regime and the “long”-time Fermi regime [15,23]. In the Zeno regime, all frequencies are excited in phase, and their photon population grows quadratically in time: this is typical of the Zeno dynamics. At longer times, it appears that only positive frequencies see their population further increase, but the increase becomes linear in time. It is well known that, in this time regime, this increase in the population of positive frequencies is driven by

the electromagnetic frequencies which are resonant with the atomic transition ω_0 .

VIII. CONCLUSION

We investigated the noncausality associated to the quantum spontaneous emission process through a detailed study of the photon wave function that characterizes the emitted photon. Our study reveals (see discussion of Sec. [VIB](#)) the existence of a blurring of the light cone that can be attributed in last resort to the spatial extension of the emitting electronic source. This should not be confused with what Einstein called “spooky action at a distance,” in which faster than light influences propagate at a large distance from the light cone. Here the noncausality vanishes exponentially over a very short distance, comparable to the size of the atom.

Beside this “tail effect” we also studied the Hegerfeldt noncausality. In order to estimate an upper bound on the strength of this other source of noncausality, we numerically studied the weight of the negative and positive frequency modes which is encapsulated in the figures of Sec. [VII](#). Having in mind that (i) the tail effect discussed in Sec. [VIB](#) is a mere consequence of the (multipolar) exact atom-field coupling, so that, in the dipole approximation, it is sufficient to consider Hegerfeldt type noncausality (ii) in the dipole approximation the sum of the positive and negative frequency contributions cancels outside the light cone, (iii) the weight of the negative frequency contributions provides an upper bound on the weight of noncausality, because in the dipole approximation the noncausal part of the wave function can be attributed solely to (the absence of) negative frequencies, it is obvious that when and where the weight of the negative frequencies is small, so is the noncausality.

It would arguably have been sufficient to limit ourselves to the far-field contributions, having in mind that we are interested in violations of causality at large distances; however, we also took account of the mid- and even near-field [[24,28,32](#)]

contributions [[33](#)] too in order to properly tackle the short time–short distance regime.

We conclude that we did not establish that causality is violated by the spontaneous emission process. At distances from the nucleus which are comparable to the size of the atom, an apparent noncausality is present, during a time short compared to the lifetime of the excitation, for which the weight of the photon wave function is small. However, after a time comparable to the lifetime of the excitation, no significant part of the wave function survives farther out of the light cone than on a distance of the order of the atomic size.

It would be highly instructive to be able to firmly derive causality from the QED Hamiltonian (as an exact result). Obviously this should be done in a Lorentz covariant approach, and would necessitate to use Dirac-Coulomb electronic wave functions instead of Schrödinger-Coulomb wave functions, as was done here. It could be the case that the perturbative approach that we followed here prohibits the derivation of such a result, and that it is necessary to resort to a more general formulation of QED, as was done for instance in Ref. [[34](#)], in the framework of axiomatic quantum field theory. It is our hope however that causality could be formulated more explicitly in terms of Green’s functions, as is the case for Maxwell’s equations, but this apparently simple question is still open today.

ACKNOWLEDGMENTS

V.D. acknowledges support from Centre National de la Recherche Scientifique (CNRS) (INSIS doctoral grant). T.D. acknowledges support from the European Cooperation of Science and Technology (COST) 1006 and COST 1403 actions. We thank Prof. Édouard Brainis for helpful discussions. We also thank Nikolai Korchagin at the Joint Institute for Nuclear Research in Dubna for sending us a copy of Shirokov’s paper [[30](#)]. Very warm thanks go to Vladyslav Atavin who sat down with one of us (V.D.) to translate Shirokov’s paper [[30](#)] from Russian.

-
- [1] E. Fermi, *Rev. Mod. Phys.* **4**, 87 (1932).
 - [2] M. Shirokov, *Sov. Phys. Usp.* **21**, 345 (1978).
 - [3] A. K. Biswas, G. Compagno, G. M. Palma, R. Passante, and F. Persico, *Phys. Rev. A* **42**, 4291 (1990).
 - [4] G. C. Hegerfeldt, *Phys. Rev. Lett.* **72**, 596 (1994).
 - [5] J. Sipe, *Phys. Rev. A* **52**, 1875 (1995).
 - [6] V. Weisskopf and E. Wigner, *Z. Phys.* **63**, 54 (1930).
 - [7] R. Paley and N. Wiener, *Fourier Transforms in the Complex Domain* (The American Mathematical Society, Providence, RI, 1934).
 - [8] Note that in Refs. [[1–4](#)] the authors consider not one atom in free space but two, the first one being initially in its excited state while the second one starts in its ground state. Rather than computing the emitted field, they focus on the probability of excitation of the second atom as a function of time (this is known in the literature as the “Fermi problem”). Our present study features a single atom, initially in its excited state, and purports to obtain the space-time dependence of the spontaneously emitted field, expressed by Glauber’s photon wave function.
 - [9] J. Seke, *Physica A* **203**, 269 (1994).
 - [10] P. Facchi, Quantum Time Evolution: Free and Controlled Dynamics, Ph.D. thesis, Università degli Studi di Bari, 2000.
 - [11] M. Scully and M. Zubairy, *Quantum Optics* (Cambridge University Press, Cambridge, UK, 1997).
 - [12] C. Cohen-Tannoudji, J. Dupont-Roc, and G. Grynberg, *Photons et atomes—Introduction à l’électrodynamique quantique*, 2nd ed. (EDP Sciences/CNRS Éditions, Paris, 2001).
 - [13] S. Weinberg, *The Quantum Theory of Fields*, 1st ed. (Cambridge University Press, Cambridge, UK, 1995), Vol. 1.
 - [14] C. Itzykson and J. Zuber, *Quantum Field Theory*, 1st ed. (McGraw-Hill, New York, 1980).
 - [15] V. Debievre, I. Goessens, E. Brainis, and T. Durt, *Phys. Rev. A* **92**, 023825 (2015).
 - [16] A. Akhiezer and V. Berestetskii, in *Quantum Electrodynamics*, 2nd ed., edited by R. Marshak (Interscience Publishers, New York, 1965).
 - [17] I. Białynicki-Birula, *Prog. Opt.* **36**, 245 (1996).
 - [18] M. Hawton, *Phys. Rev. A* **78**, 012111 (2008).
 - [19] B. Smith and M. Raymer, *New J. Phys.* **9**, 414 (2007).
 - [20] U. Titulaer and R. Glauber, *Phys. Rev.* **145**, 1041 (1966).

- [21] P. Facchi and S. Pascazio, *Phys. Lett. A* **241**, 139 (1998).
- [22] W. Appel, *Mathematics for Physics & Physicists*, 1st ed. (Princeton University Press, Princeton, NJ, 2007).
- [23] V. Debierre, T. Durt, A. Nicolet, and F. Zolla, *Phys. Lett. A* **379**, 2577 (2015).
- [24] B. Stout, V. Debierre, and T. Durt (unpublished).
- [25] M. Abramowitz and I. Stegun, *Handbook of Mathematical Functions with Formulas, Graphs, and Mathematical Tables* (Dover, New York, 1964).
- [26] This was also true of the integrals $H_{n(\text{std})}^{(\pm)}$ for $n = 1, 2$ in the $\hat{\mathbf{E}} \cdot \hat{\mathbf{x}}$ case of the previous Sec. IV.
- [27] Note that it is very easy to show that if, instead of this time-dependent perturbation theory, we plug in the expression from the usual Wigner-Weisskopf approximation [which has been shown [21] to provide a very good approximation to the dynamics of the system (except at very short times), up to very small corrections], our results for the matrix elements of the electric field hold, with a grain of salt: ω_0 should be replaced by $\omega_0 + \omega_{LS} - (i/2)\Gamma$. Therefore, our perturbative treatment works directly at short times and indirectly (through the substitution which we just specified) at intermediate times. It only fails at very long times, where the decay becomes nonexponential [21].
- [28] V. Debierre and T. Durt, Mid- and far-field deviations from causality in spontaneous light emission by atomic Hydrogen, [arXiv:1509.01475](https://arxiv.org/abs/1509.01475).
- [29] It is only if the dipole approximation is performed that the emission can be considered to take place at $\mathbf{x} = \mathbf{0}$. As discussed at length in Refs. [15,23], and also below (39), the dipole approximation results in divergences coming from ultraviolet frequencies. A possibility is then to implement a cutoff on high frequencies (the cutoff being of order c/a_0) which, of course, will induce a “blurring” of the light cone over distances of order a_0 , in virtue of the Paley-Wiener properties of the Fourier transform. In this sense, the noncausality due to the finite size of the decaying electron, first noticed by Shirokov [2] and described here in detail, is similar to Hegerfeldt’s noncausality.
- [30] M. Shirokov, JINR Report No. 1719, 1964 (unpublished).
- [31] V. Debierre, G. Demésy, T. Durt, A. Nicolet, B. Vial, and F. Zolla, *Phys. Rev. A* **90**, 033806 (2014).
- [32] V. Debierre The Photon Wave Function in Principle and in Practice, Ph.D. thesis, École Centrale de Marseille, 2015.
- [33] In Ref. [28], extra material is presented where we study the noncausality in the near field, as well as Hegerfeldt type noncausality in the case where no dipolar approximation is made. In an upcoming manuscript [24] we will focus particularly on the near field, where the longitudinal (in the sense of Fourier space, see [12]) contribution to the electric field comes into play.
- [34] D. Buchholz and J. Yngvason, *Phys. Rev. Lett.* **73**, 613 (1994).